

Supporting Information for

Field-Induced Slow Relaxation of Two 1-D Compounds Containing Six-coordinated Cobalt(II) Ions: Influence of the Coordination Geometry

*Zhiwei Chen^{a‡}, Lei Yin^{c‡}, Xiuna Mi^a, Suna Wang^{*a}, Fan Cao^{*b}, Zhenxing*

*Wang^{*c}, Yunwu Li^a, Jing Lu^a, Jianmin Dou^a*

^aShandong Provincial Key Laboratory of Chemical Energy Storage and Novel Cell
Technology, School of Chemistry and Chemical Engineering, Liaocheng University,
Liaocheng, 252059, P. R. China.

^bQingdao University of Science & Technology, College of Chemistry and Molecular
Engineering, 266042, P. R. China.

^cWuhan National High Magnetic Field Center & School of Physics, Huazhong
University of Science and Technology, Wuhan, Hubei, 430074, P.R. China.

Table of contents.

Table S1. The selected bond lengths and angles of compounds **1** and **2**.

Table S2 .Results of Continuous Shape Measure Analysis for $\text{CoO}_4\text{N}_2^{2+}$ units in compounds **1** and **2**^a

Table S3. The relaxation fitting parameters from Least-Squares Fitting of $\chi(\omega)$ data for compound **1** from 2.2 to 6.0 K under 2 kOe dc field.

Table S4. The relaxation fitting parameters from Least-Squares Fitting of $\chi(\omega)$ data for compound **2** from 2.2 to 6.0 K under 2 kOe dc field.

Fig. S1 (a) View of the 3-D supramolecular structure of compound **1** along the c axis, showing the $\pi \cdots \pi$ interactions between the aromatic rings of the neighboring chains. (b) The C-H \cdots O interactions between neighboring chains.

Fig. S2 (a) View of the 3-D supramolecular structure of compound **2** along the a axis. (b) View of hydrogen bonding interactions between the carboxylate oxygen atoms of the uncoordinated L2 ligand and coordinated aqua molecules of the neighboring chains along the ab plane.

Fig.S3 The temperature dependence of the in-phase (χ') and out-of-phase (χ'') ac susceptibilities at different frequencies with zero dc field for compounds **1**(a) and **2** (b), respectively.

Fig.S4 Arrhenius plots of relaxation times of **1** under 2000 Oe dc field, the data was collected from the peaks of χ'' (out-of-phase) against frequency at different temperature.

Fig. S5 Plots of $\ln(\chi''/\chi')$ versus $1/T$ of compound **2**. The solid lines represent the fitting results.

Fig. S6 HF-EPR spectra of compounds **1** (a) and **2** (b) at 4.2 K and various frequencies. The spectra are offset in proportion to the frequency. Black dots represent the resonance fields for each spectrum.

Table S1. The selected bond lengths and angles of compounds **1** and **2**.

Compound 1			
Co(1)-O(1)	2.076(3)	N(1)-Co(1)-N(2)	77.43(17)
Co(1)-O(2)	2.197(3)	O(4)-Co(1)-O(2)	102.40(12)
Co(1)-O(3)	2.212(3)	O(1)-Co(1)-O(2)	61.04(12)
Co(1)-O(4)	2.065(3)	N(1)-Co(1)-O(2)	149.69(15)
Co(1)-N(1)	2.099(5)	O(1)-Co(1)-O(3)	102.31(12)
Co(1)-N(2)	2.100(4)	N(1)-Co(1)-O(3)	91.62(14)
O(4)-Co(1)-O(1)	152.33(12)	N(2)-Co(1)-O(2)	88.50(15)
O(4)-Co(1)-N(1)	105.98(16)	O(4)-Co(1)-O(3)	61.15(12)
O(1)-Co(1)-N(1)	95.96(16)	N(2)-Co(1)-O(3)	152.93(15)
O(4)-Co(1)-N(2)	97.78(14)	O(2)-Co(1)-O(3)	111.48(11)
O(1)-Co(1)-N(2)	103.39(14)		
Compound 2			
Co(1)-O(4)	2.059(4)	O(4)-Co(1)-N(2)	89.93(18)
Co(1)-O(4)	2.059(4)	O(4)-Co(1)-N(2)	90.07(18)
Co(1)-O(5)	2.127(4)	O(5)-Co(1)-N(2)	86.35(14)
Co(1)-O(5)	2.127(4)	O(5)-Co(1)-N(2)	93.65(14)
Co(1)-N(2)	2.183(4)	O(4)-Co(1)-N(2)	90.07(18)
Co(1)-N(2)	2.183(4)	O(4)-Co(1)-N(2)	89.93(18)
O(4)-Co(1)-O(4)	180.000(1)	O(5)-Co(1)-N(2)	93.65(14)
O(4)-Co(1)-O(5)	91.33(18)	O(5)-Co(1)-N(2)	86.35(14)
O(4)-Co(1)-O(5)	88.67(17)	N(2)-Co(1)-N(2)	180.000(1)
O(4)-Co(1)-O(5)	88.67(18)	C(14)-N(2)-Co(1)	120.3(4)
O(4)-Co(1)-O(5)	91.33(18)	C(15)-N(2)-Co(1)	134.2(3)
O(5)-Co(1)-O(5)	180		

Table S2 .Results of Continuous Shape Measure Analysis for $\text{CoO}_4\text{N}_2^{2+}$ units in compounds **1** and **2**^a

Geometry	HP-6	PPY-6	OC-6	TPR-6	JPPY-6	configuration
Compound 1	32.111	18.693	6.818	7.269	22.673	Intermediate OC-6/TPR-6
Compound 2	31.424	29.163	0.134	16.266	32.386	OC-6

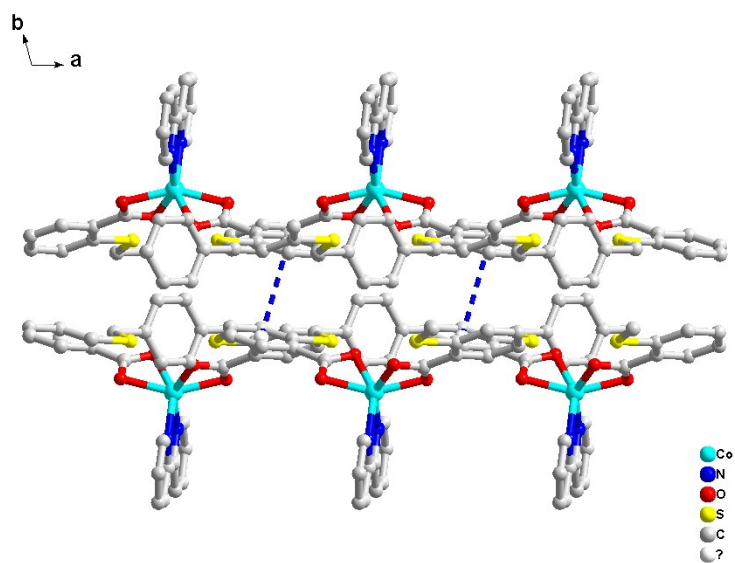
^a The values are Continuous Shape Measure (CShM) parameters and CShM=0 for the ideal geometry and increases with the degree of distortion; HP-6 corresponds to the hexagon geometry; PPY-6 corresponds to the pentagonal pyramid geometry; OC-6 corresponds to the octahedron geometry; TPR-6 corresponds to the trigonal prism geometry; JPPY-6 corresponds to the Johnson pentagonal pyramid (J2) geometry.

Table S3. The relaxation fitting parameters from Least-Squares Fitting of $\chi(\omega)$ data for compound **1** from 2.2 to 6.0 K under 2 kOe dc field.

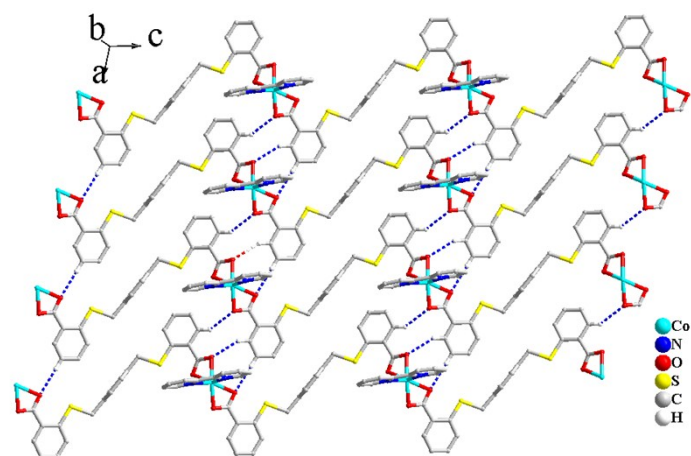
T	χ_s	χ_T	τ	α
2.2	0.0195	0.856	0.00161	0.192
2.4	0.0203	0.808	0.00130	0.181
2.6	0.0171	0.766	0.00103	0.175
2.8	0.0158	0.725	0.000793	0.165
3.0	0.0117	0.687	0.000592	0.159
3.5	0.330×10^{-9}	0.608	0.000270	0.165
4.0	0.470×10^{-9}	0.543	0.000126	0.165
4.5	0.898×10^{-9}	0.489	0.653×10^{-4}	0.135
5.0	0.162×10^{-10}	0.443	0.375×10^{-4}	0.0776
5.5	0.225×10^{-9}	0.404	0.233×10^{-4}	0.0201
6.0	0.725×10^{-22}	0.372	0.145×10^{-4}	0.46×10^{-15}

Table S4. The relaxation fitting parameters from Least-Squares Fitting of $\chi(\omega)$ data for compound **2** from 2.2 to 6.0 K under 2 kOe dc field.

T	χ_s	χ_T	τ	α
2.2	0.169×10^{-14}	0.772	0.569×10^{-4}	0.155
2.6	0.253×10^{-14}	0.692	0.438×10^{-4}	0.118
3.0	0.263×10^{-15}	0.624	0.337×10^{-4}	0.102
3.5	0.323×10^{-15}	0.551	0.258×10^{-4}	0.0728
4.0	0.707×10^{-15}	0.492	0.201×10^{-4}	0.0588
5.0	0.952×10^{-15}	0.403	0.134×10^{-4}	0.0355
6.0	0.158×10^{-14}	0.341	0.102×10^{-4}	0.00322

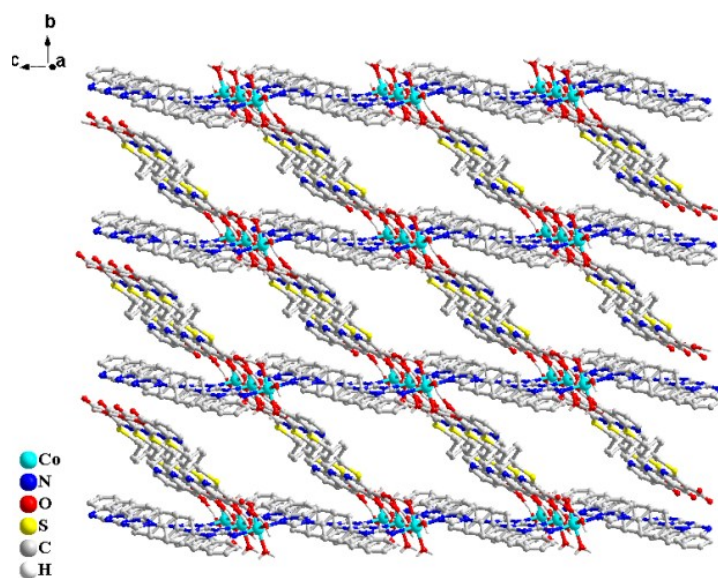


(a)

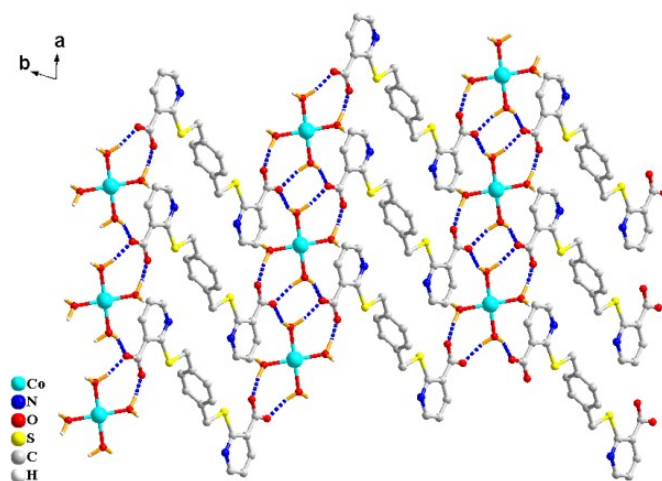


(b)

Fig. S1 (a) View of the 3-D supramolecular structure of compound **1** along the c axis, showing the $\pi \cdots \pi$ interactions between the aromatic rings of the neighboring chains. (b) The C-H \cdots O interactions between neighboring chains.

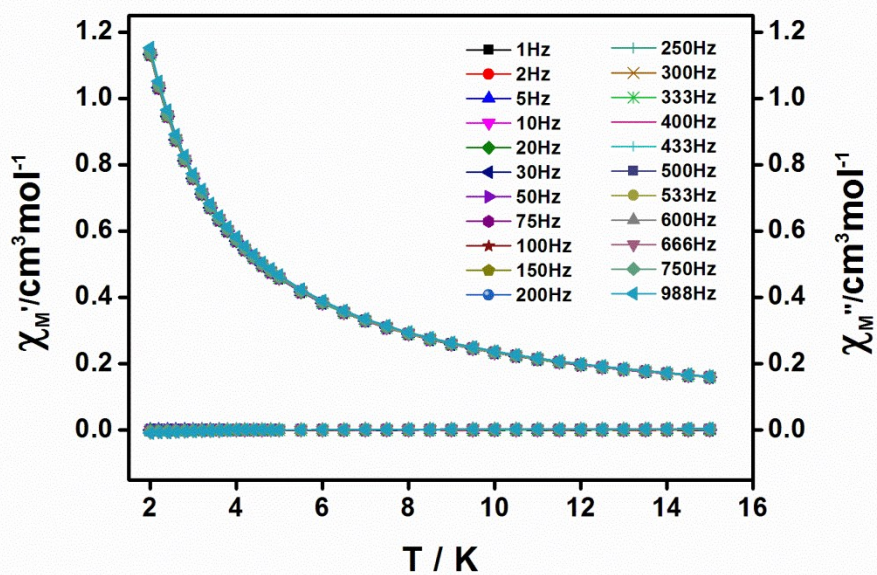


(a)

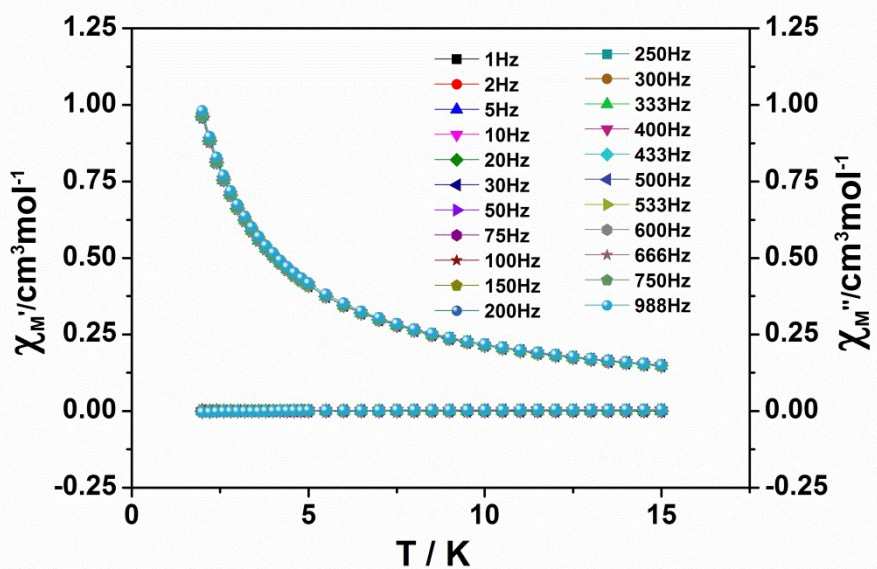


(b)

Fig. S2 (a) View of the 3-D supramolecular structure of compound **2** along the a axis. (b) View of hydrogen bonding interactions between the carboxylate oxygen atoms of the uncoordinated L2 ligand and coordinated aqua molecules of the neighboring chains along the ab plane.



(a)



(b)

Fig.S3 The temperature dependence of the in-phase (χ') and out-of-phase (χ'') ac susceptibilities at different frequencies with zero dc field for compounds 1(a) and 2 (b), respectively.

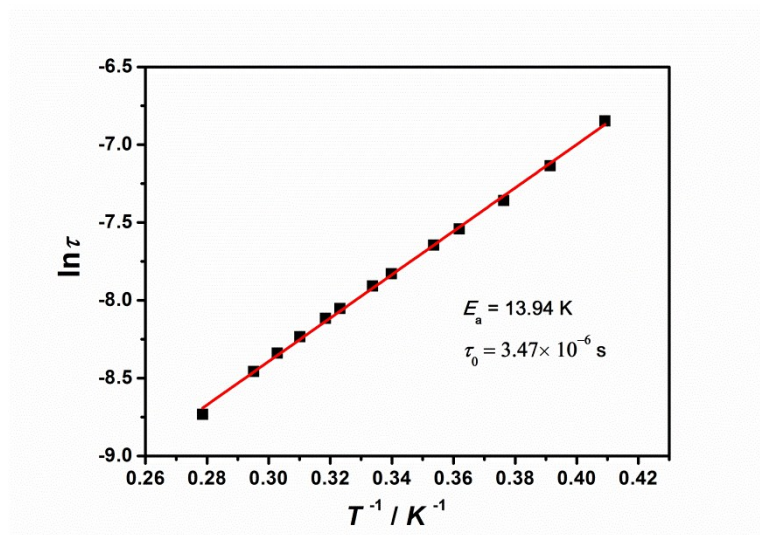


Fig.S4 Arrhenius plots of relaxation times of **1** under 2000 Oe dc field, the data was collected from the peaks of χ'' (out-of-phase) against frequency at different temperature.

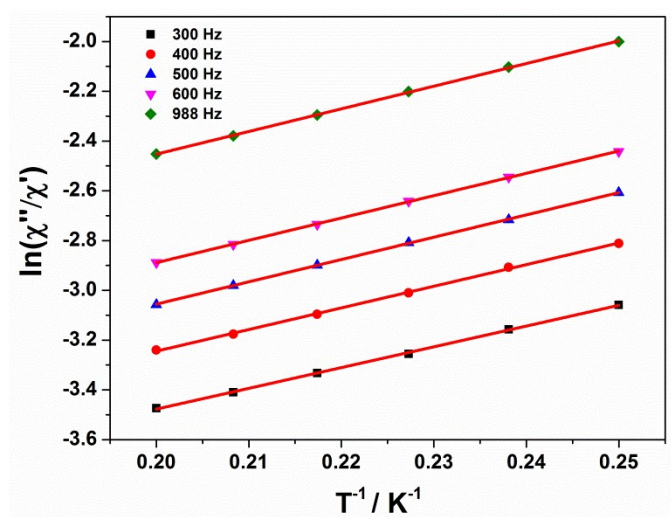


Fig. S5 Plots of $\ln(\chi''/\chi')$ versus $1/T$ of compound **2**. The solid lines represent the fitting results.

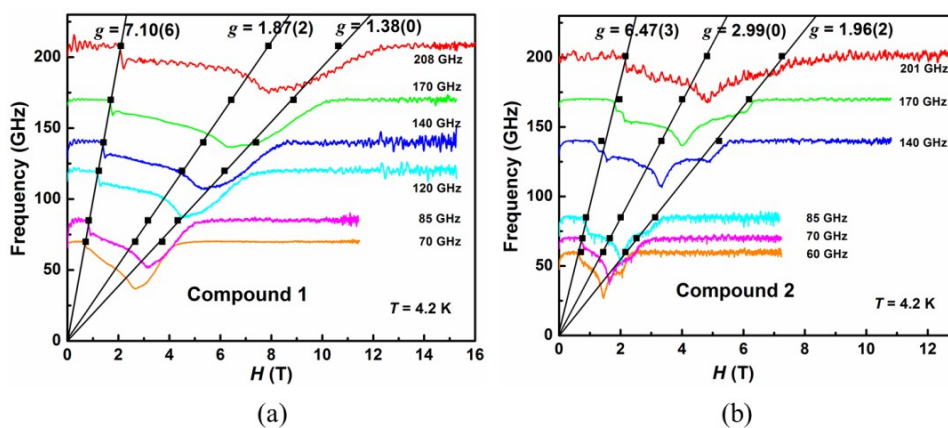


Fig. S6 HF-EPR spectra of compounds 1 (a) and 2 (b) at 4.2 K and various frequencies. The spectra are offset in proportion to the frequency. Black dots represent the resonance fields for each spectrum.